

SUPPLEMENTARY MATERIAL
for
Multi-Material Decomposition Using Statistical Image
Reconstruction for Spectral CT

Yong Long and Jeffrey A. Fessler, Fellow, IEEE

April 23, 2014

1 Generalized Sequential Minimization Algorithm (GSMO) for Optimization with Given Material Types

The Generalized Sequential Minimization Algorithm (GSMO) [1] was proposed originally for solving quadratic programming problems arising in support vector machines. The GSMO is derived using Karush-Kuhn-Tucker (KKT) conditions, guaranteed to converge and significantly faster than the original SMO [1].

For simplification of notation, we drop the notations on iteration (n), pixel index j and material triplet ω , and write the quadratic optimization problem with constraints in equation (47) of this paper as

$$\begin{aligned} \hat{\mathbf{x}} &= \arg \min_{\mathbf{x}} \phi(\mathbf{x}) \\ \phi(\mathbf{x}) &\equiv \frac{1}{2} \mathbf{x}' \mathbf{H} \mathbf{x} + \mathbf{p}' \mathbf{x} \\ \text{s.t.} &\quad \begin{cases} \sum_{l=1}^L x_l = 1, \\ a_l \leq x_l \leq b_l. \end{cases} \end{aligned} \quad (1)$$

Table 1 summarizes the pseudo-code of GSMO for solving (1). Please refer to the original GSMO publication [1] for details and derivations of this algorithm. The algorithm is available in the image reconstruction toolbox online [2].

2 Supplementary Figures

Fig. 1 shows the fraction images reconstructed by the ID method [3] without median filtering. Fig. 2, Fig. 3, Fig. 4 and Fig. 5 show profiles of reconstructed fat, blood, bone and air component fraction images by the filtered ID method and the PL method.

References

- [1] S. S. Keerthi and E. G. Gilbert. Convergence of a generalized SMO algorithm for SVM classifier design. *Machine Learning*, 46(1-3):351–60, 2002.

1. Choose a tolerance parameter $\tau > 0$.
2. Initialize $k = 0$ and $\hat{\mathbf{x}}^{(0)} \in \mathcal{F}$ where \mathcal{F} denotes the feasible set of (1).

3. **Repeat**

- (a) Compute derivatives of $\phi(\hat{\mathbf{x}}^{(k)})$

$$F_l^{(k)} = [\mathbf{H}\hat{\mathbf{x}}^{(k)} + \mathbf{p}]_l$$

- (b) Update the following index sets

$$\mathcal{I}_0^{(k)} = \{l : a_l < [\hat{\mathbf{x}}^{(k)}]_l < b_l\}, \quad \mathcal{I}_1^{(k)} = \{l : a_l = [\hat{\mathbf{x}}^{(k)}]_l\}, \quad \mathcal{I}_2^{(k)} = \{l : b_l = [\hat{\mathbf{x}}^{(k)}]_l\}$$

$$\mathcal{I}_{\text{up}}^{(k)} = \mathcal{I}_0^{(k)} \cup \mathcal{I}_1^{(k)}, \quad \mathcal{I}_{\text{low}}^{(k)} = \mathcal{I}_0^{(k)} \cup \mathcal{I}_2^{(k)}$$

- (c) Find the most τ -violating index pair (m, n) as

$$m = m^{(k)} = \arg \min_{l \in \mathcal{I}_{\text{up}}^{(k)}} F_l^{(k)}, \quad n = n^{(k)} = \arg \max_{l \in \mathcal{I}_{\text{low}}^{(k)}} F_l^{(k)}$$

- (d) Minimize $\phi(\hat{\mathbf{x}})$ on \mathcal{F} while varying only (x_m, x_n) and update them with the minimizer.

$$\hat{x}_m^{(k+1)} = \hat{x}_m^{(k)} + t, \quad \hat{x}_n^{(k+1)} = \hat{x}_n^{(k)} - t,$$

where

$$t = \min \left(\max \left(\frac{F_m^{(k)} - F_n^{(k)}}{[\mathbf{H}]_{mm} + [\mathbf{H}]_{nn} - 2[\mathbf{H}]_{mn}}, t_1 \right), t_2 \right),$$

$$t_1 = \max \left(a_m - \hat{x}_m^{(k)}, \hat{x}_n^{(k)} - b_n \right), \quad t_2 = \min \left(b_m - \hat{x}_m^{(k)}, \hat{x}_n^{(k)} - a_n \right)$$

- (e) $k = k + 1$

Until $\hat{\mathbf{x}}_j^{(k)}(\omega)$ satisfies the KKT condition

$$\min_{l \in \mathcal{I}_{\text{up}}^{(k)}} F_l^{(k)} \geq \max_{l \in \mathcal{I}_{\text{low}}^{(k)}} F_l^{(k)} - \tau$$

4. Minimizer $\hat{\mathbf{x}} = \hat{\mathbf{x}}^{(k)}$

Table 1: Pseudo-code of GSMO for solving the quadratic optimization problem with constraints in (1).

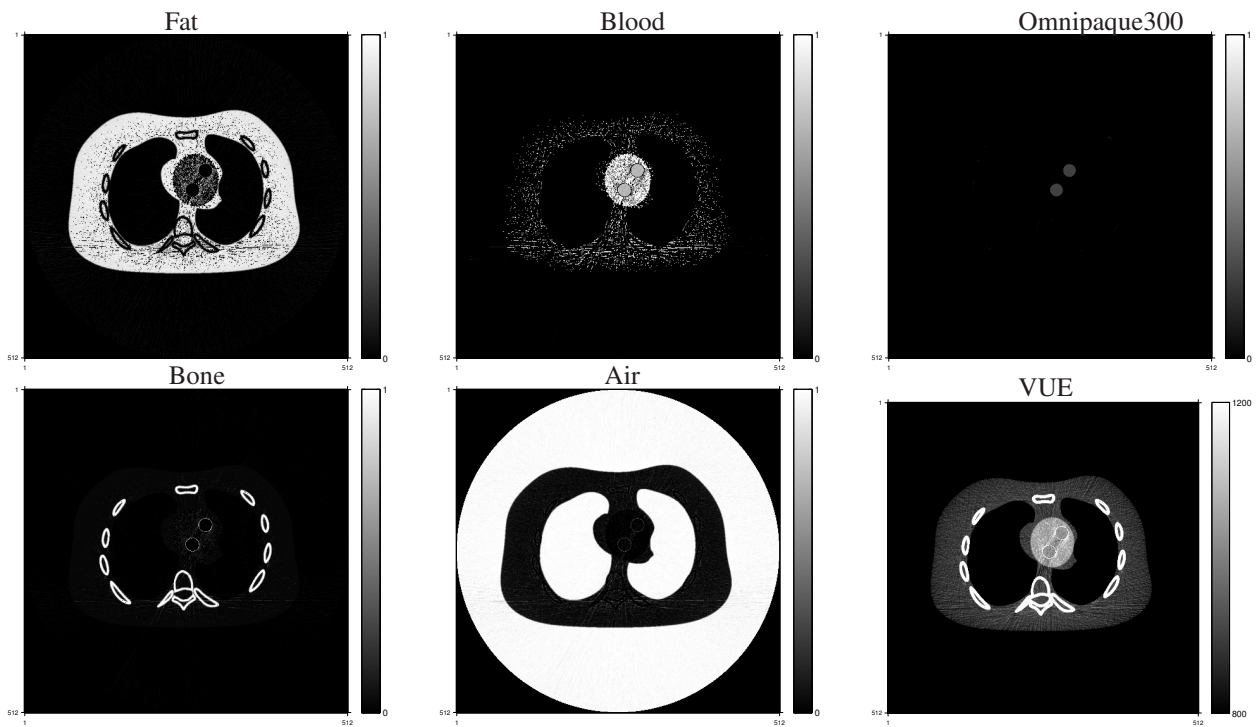


Figure 1: Reconstructed volume fractions of five component images and VUE image at 70 keV by the ID method. The volume fractions are in the range of $[0, 1]$ and the monoenergetic image is displayed over $[800, 1200]$ with the shifted Hounsfield unit (HU) scale where air is 0 HU and water is 1000 HU.

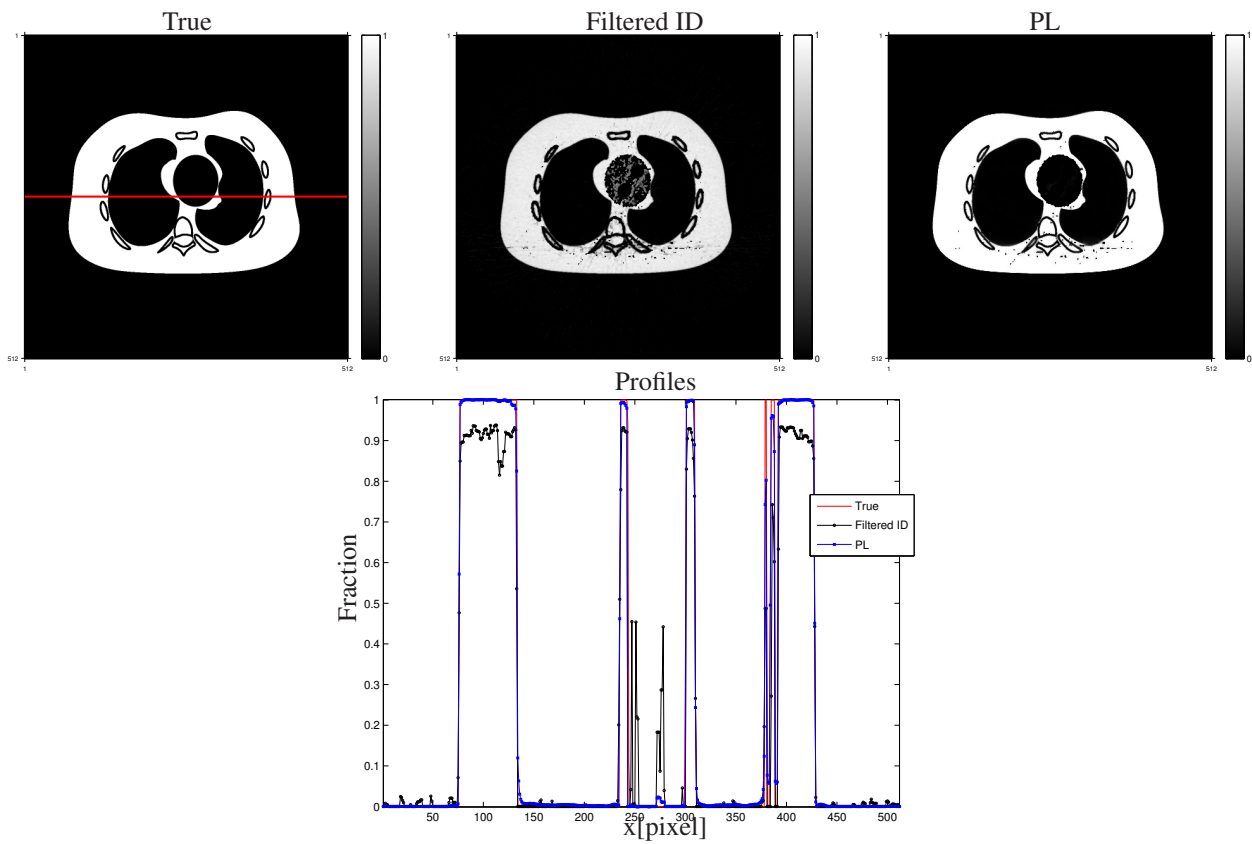


Figure 2: Fat component fraction images reconstructed by the filtered ID method (*upper center*) and the PL method (*upper right*). The upper left image is the down-sampled true image. The lower image shows the horizontal profiles through the red line in the down-sampled true image.

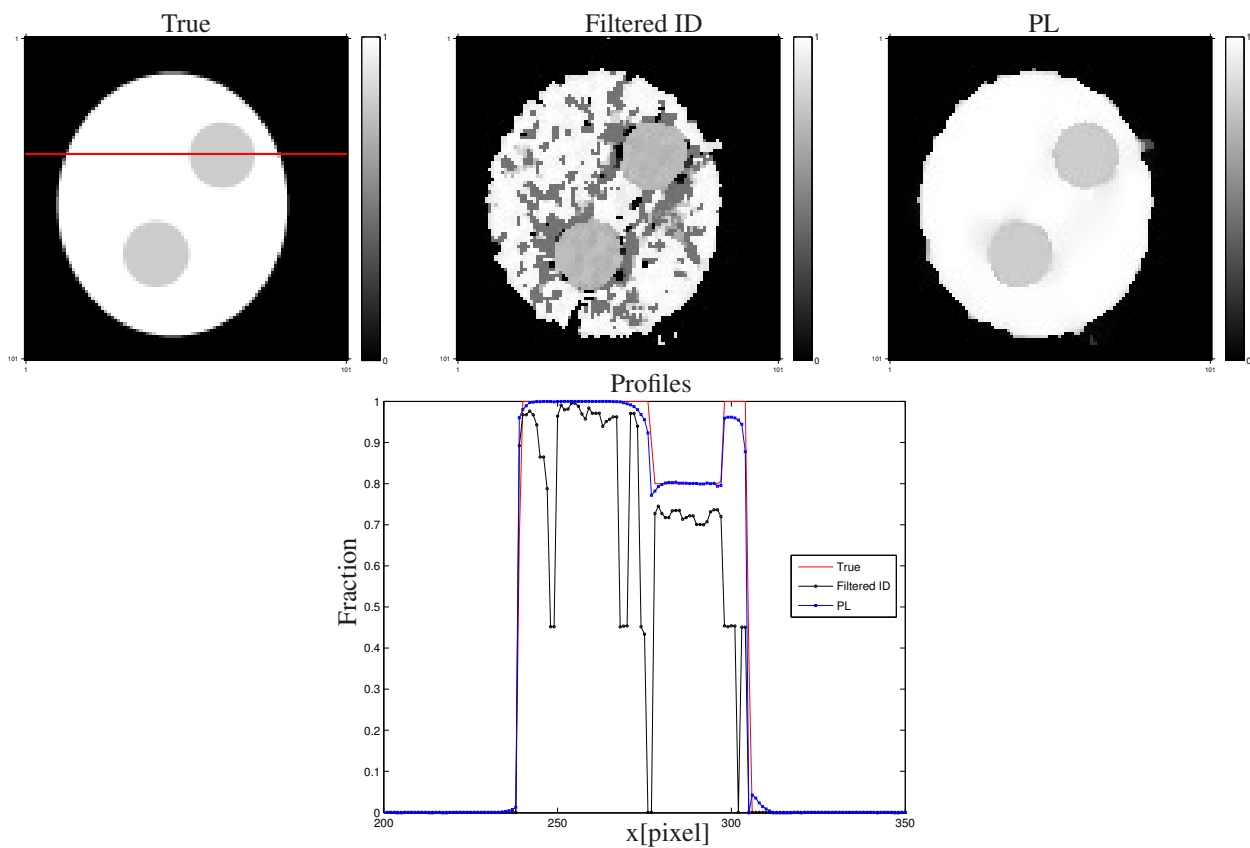


Figure 3: Zoom-in blood component fraction images reconstructed by the filtered ID method (*upper center*) and the PL method (*upper right*). The upper left image is the down-sampled true image. The lower image shows the horizontal profiles through the red line in the down-sampled true image.

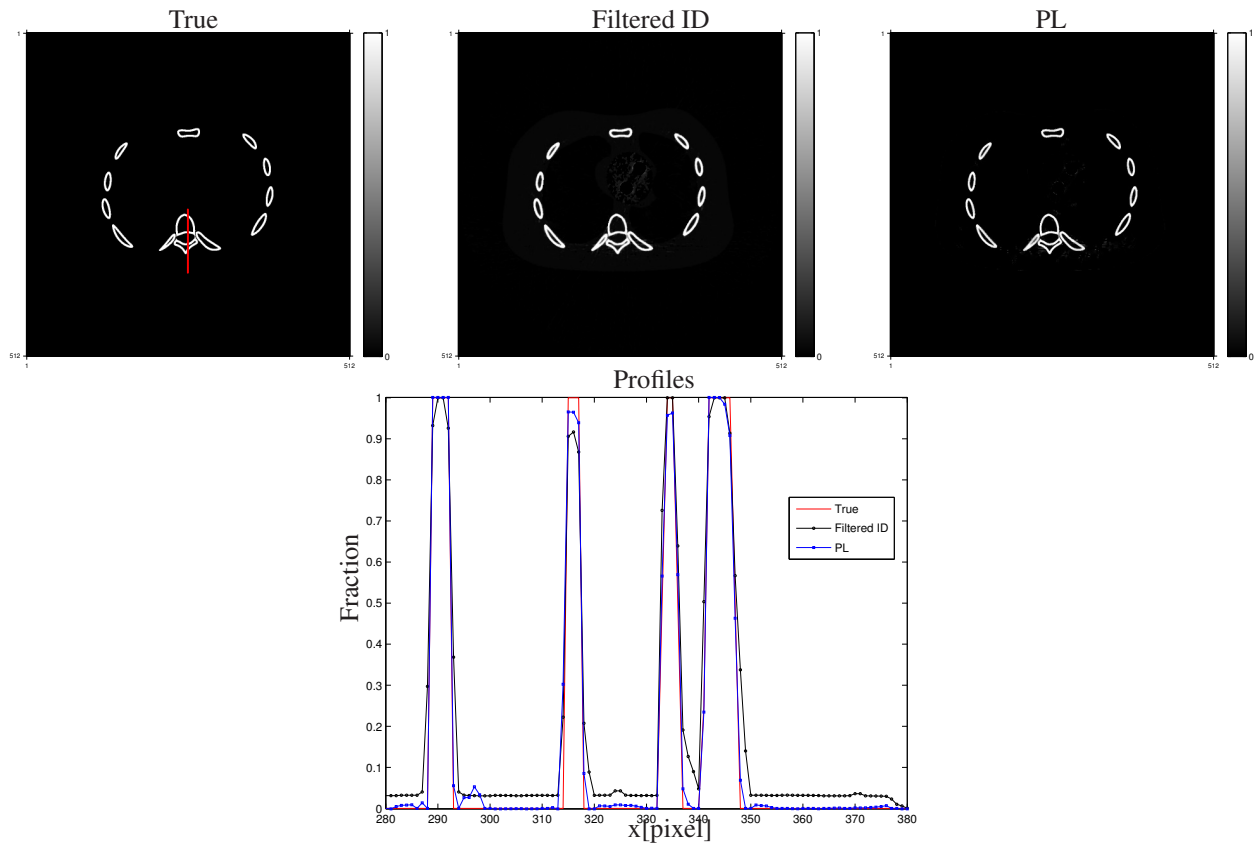


Figure 4: Cortical bone component fraction images reconstructed by the filtered ID method (*upper center*) and the PL method (*upper right*). The upper left image is the down-sampled true image. The lower image shows the vertical profiles through the red line in the down-sampled true image.

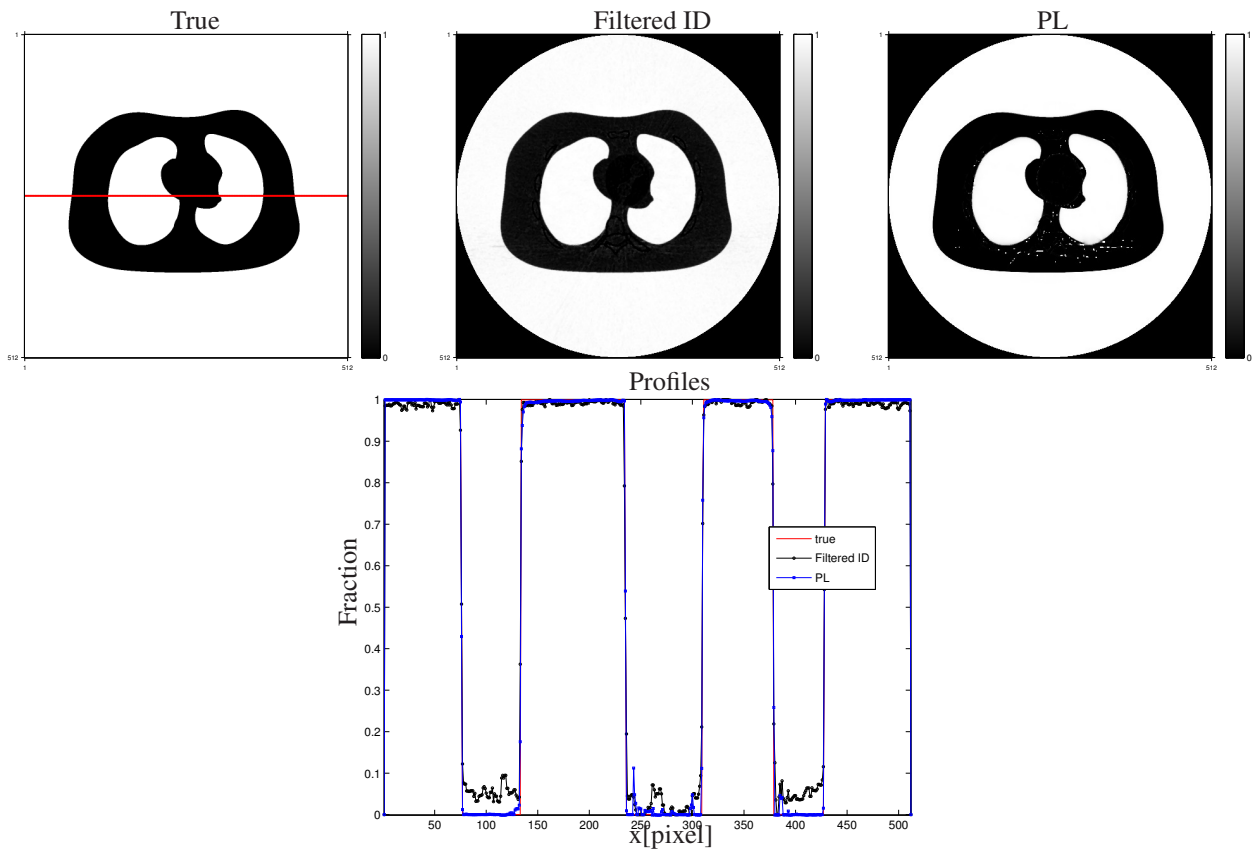


Figure 5: Air component fraction images reconstructed by the filtered ID method (*upper center*) and the PL method (*upper right*). The upper left image is the down-sampled true image. The lower image shows the horizontal profiles through the red line in the down-sampled true image.

- [2] J. A. Fessler. Matlab tomography toolbox, 2004. Available from <http://www.eecs.umich.edu/~fessler>.
- [3] P. R. S. Mendonca, P. Lamb, and D. Sahani. A flexible method for multi-material decomposition of dual-energy CT images. *IEEE Trans. Med. Imag.*, 33(1):99–116, January 2014.